The Art of Modelling Stars in the 21st Century
Proceedings IAU Symposium No. 252, 2008
L.Deng & K.L.Chan, eds.

doi:10.1017/S1743921308022710

Deep inside low-mass stars

Corinne Charbonnel[1,2] and Suzanne Talon[3]

[1]Geneva Observatory, University of Geneva, ch. des Maillettes 51, 1290 Versoix, Switzerland
email: Corinne.Charbonnel@obs.unige.ch

[2]Laboratoire d'Astrophysique de Toulouse-Tarbes, Université de Toulouse, CNRS UMR 5572, 14 Av. E.Belin, 31400 Toulouse, France

[3]RQCHP, Département de physique, Université de Montréal, C. P. 6128, succ. centre-ville, Montréal, Québec, H3C 3J7
email: talonsuz@rqchp.qc.ca

Abstract. Low-mass stars exhibit, at all stages of their evolution, the signatures of complex physical processes that require challenging modeling beyond standard stellar theory. In this review, we recall the most striking observational evidences that probe the interaction and interdependence of various transport processes of chemicals and angular momentum in these objects. We then focus on the impact of atomic diffusion, large scale mixing due to rotation, and internal gravity waves on stellar properties on the main sequence and slightly beyond.

Keywords. hydrodynamics - instabilities - turbulence - waves - stars: abundances- stars: evolution - stars: interiors - stars: rotation

1. Clues on transport processes in low-mass stars

During the last couple of decades, it became obvious that "the art of modeling stars in the 21st century" will actually strongly rely on the art of modeling transport processes in stars. Observational evidences now give precise clues on the various processes that transport angular momentum and chemical elements in the radiative regions of low-mass stars, at various phases of their evolution. Here are a few examples of observations that require modeling beyond standard stellar theory: The abundance patterns of lithium in the Sun, in field and cluster main sequence and subgiant stars, as well as in Population II dwarfs; the rotation profile in the Sun inferred from helioseismology; the abundance patterns of lithium, beryllium, carbon and nitrogen on the red giant branch (see Charbonnel & Zahn 2007a, b, and this volume); the intrinsic s-process elements observed in AGB stars; the abundance of helium 3 and heavier elements in planetary nebulae; the observed spin of white dwarfs.

One of the most striking signatures of transport processes in low-mass stars is the so-called Li dip (see Fig. 1). This drop-off in the Li content of main-sequence F-stars in a range of ∼300 K centered around 6700 K was discovered in the Hyades by Wallerstein *et al.* (1965); its existence was latter confirmed by Boesgaard & Tripicco (1986). This feature appears in all open clusters older than ∼200 Myr, as well as in field stars (Balachandran 1995), an indication that it is a phenomenon occurring on the main sequence.

It was first suggested by Michaud (1986) that the Li dip could be due to element separation below the stellar convective envelope. He showed that Li is supported by radiative acceleration at the bottom of the convective envelope in stars with $T_{\rm eff} \geqslant$ 7000 K, while gravitational settling dominates and leads to Li underabundances in stars with $T_{\rm eff}$ between 6800 and 6400 K. In cooler stars, at the age of the Hyades, atomic diffusion did not have enough time to modify the Li abundance in the deep surface

convection zone. These predictions were obtained from first principles, the only free parameter being the mixing length parameter, which controls the effective temperature of the Li dip. In addition, a mass loss rate of the order of $10^{-15} M_{\odot}\,\mathrm{yr}^{-1}$ was required to reduce the expected Li overabundance on the hot side of the dip. More sophisticated models based solely on atomic diffusion were constructed by Richer & Michaud (1993), but this explanation suffers from two serious drawbacks:

► The expected concomitant underabundances of heavier elements (C, N, O, Mg, Si) are not observed in cluster stars (Takeda *et al.* 1998; Varenne & Monier 1999; Gebran *et al.* 2008).

► In this framework Li is not destroyed; it rather settles out of the convective envelope and accumulates in a buffer zone below. As a consequence, Li should be dredged-up as a star enters the Hertzsprung gap. This is not seen in the Li data, neither in the field nor in open cluster stars (Pilachowski *et al.* 1988; Deliyannis *et al.* 1997).

This suggests that another process is responsible for the existence of the Li dip. Boesgaard (1987) noticed that the effective temperature of the dip is also associated with a sharp drop in rotation velocities as can be seen in Fig. 1. Rotation was then suggested to play a dominant role in this mass range.

2. Rotation-induced transport in low-mass stars

In order to properly model rotation-induced mixing, one must follow the time evolution of the angular momentum distribution within a star, taking into account *all* relevant physical processes: contraction/expansion caused by the stellar evolution, mass loss or accretion, tidal effects, as well as internal redistribution of angular momentum through meridional circulation, turbulence, magnetic torques, waves, etc.

As discussed by Zahn in these proceedings, the description of the internal physical processes related to stellar rotation has been greatly improved during the last two decades. Talon & Charbonnel (1998; see also Charbonnel & Talon 1999, Palacios *et al.* 2003, Pasquini *et al.* 2004, and Decressin *et al.* in preparation) showed that the hot side of the Li dip (down to $T_{\rm eff} \sim 6500$ K) is very well reproduced using Zahn's (1992) model of rotation-induced mixing and the same free parameters as those required to explain abundance anomalies in more massive stars (see Zahn, and Meynet, this volume). In this framework, transport of angular momentum is dominated by the Eddington-Sweet meridional circulation and shear instabilities. The blue side of the Li dip is then attributed to enhanced mixing (and thus, Li burning) caused by the large angular momentum gradients created by surface braking. However these rotating models fail to reproduce the Li rise on the cool side of the dip, i.e., for stars with effective temperature lower than ∼6600 K. Why is it so?

This effective temperature appears to be a "pivotal" value in the rotation history of stars (see Fig. 1). Indeed, the physical processes responsible for the evolution of the surface velocity are different on each side of the Li dip, and the plot may be split into three temperature ranges associated with different dominant physical processes:

► Stars with $T_{\rm eff}$ higher than ∼6900 K have a very shallow convective envelope, which is not an efficient site for magnetic generation via a dynamo process†. Thus, contrary to Sun-like stars, they are not slowed down by a magnetic torque. As a result, these stars soon reach a stationary regime where there is no net flux of angular momentum‡, in which

† Here, we discuss the presence of an "external" magnetic field, which could interact with mass loss.

‡ In fact, there remains a small flux of angular momentum, just sufficient to counteract the effect of stellar contraction/expansion.

https://doi.org/10.1017/S1743921308022710 Published online by Cambridge University Press

meridional circulation and turbulence counterbalance each other. The associated weak mixing is just sufficient to counteract atomic diffusion. These rotating models account nicely for the observed constancy of Li and CNO in these stars, and they also explain the Li behaviour in subgiant stars (Palacios *et al.* 2003; Pasquini *et al.* 2004).

In this region Am stars, which are known to be slow rotators, offer very good constraints to probe the processes that compete with atomic diffusion (e.g., Richer *et al.* 2000). Talon, Richard, & Michaud (2006) showed that the transport coefficients related to rotation-induced mixing lead to normal A stars for rotation velocities above $\sim$100 km s^{-1}, and permit Am anomalies below, with a mild correlation with rotation, provided a reduction of turbulent mixing by horizontal turbulence is taken into account. Fossati *et al.* (2008) have confirmed observationally this correlation with rotation: in a large sample of stars in Praesepe, they find indeed a strong correlation between chemical pecularities of Am stars and their $v \sin i$.

► Between $\sim$6900 and 6600 K, the convective envelope deepens and a weak magnetic torque, associated with the appearing dynamo, spins down the outer layers of the star. In this case, the transport of angular momentum by meridional circulation and shear turbulence increases, leading to a larger destruction of Li, in agreement with the data. The rotating model thus perfectly fits the blue side of the Li dip.

► Stars on the cool side of the Li dip ($T_{\rm eff} < 6600$ K) have an even deeper convective envelope sustaining a very efficient dynamo, which produces a strong magnetic torque that spins down the outer layers very efficiently. If we assume that all the angular momentum transport is assured by the wind-driven circulation in these stars†, we obtain too much Li depletion compared to the observations (see Fig. 2). On the basis of these results, Talon & Charbonnel (1998) suggested that the Li dip corresponds to a transition region where another internal process starts to efficiently transport angular momentum.

This proposition is directly linked to another observation that fails to be reproduced by the pure hydrodynamic models, namely the flat solar rotation profile revealed by helioseismology (Brown *et al.* 1989; Kosovichev *et al.* 1997; Couvidat *et al.* 2003; Garcia *et al.* 2007; see also Christensen-Daalsgard, this volume). At the solar age indeed, models relying only on turbulence and meridional circulation for momentum transport predict large angular velocity gradients that are not present in the Sun (Pinsonneault *et al.* 1989; Chaboyer *et al.* 1995; Talon 1997; Matias & Zahn 1998). This is an additional clue that another process participates to the transport of angular momentum in solar-type stars.

Two mechanisms have been proposed to explain the near uniformity of the solar rotation profile. The first rests on the possible existence of a magnetic field within the radiation zone (Charbonneau & MacGregor 1993; Eggenberger *et al.* 2005). The second invokes traveling internal gravity waves (hereafter IGWs) generated at the base of the convection envelope (Schatzman 1993; Zahn *et al.* 1997; Kumar & Quataert 1997; Talon *et al.* 2002). For either of these solutions to be convincing, they must be tested with numerical models coupling these processes with rotational instabilities and should explain all the aspects of the problem, including the lithium evolution with time.

In the case of the magnetic field, two different models have been suggested. First, in a series of 2–D numerical calculations based on a static poloidal field fully contained in the Sun's radiative zone, it has been shown that, at low latitudes, radial differential rotation can be severely limited (Charbonneau & MacGregor 1993; MacGregor & Charbonneau 1999). Shear is also reduced in these models, and, for the solar case, lithium burning could be reconciled with observations (Barnes *et al.* 1999). The temperature

† Let us mention that in the case of large shears meridional circulation is far more efficient than shear for angular momentum transport.

https://doi.org/10.1017/S1743921308022710 Published online by Cambridge University Press

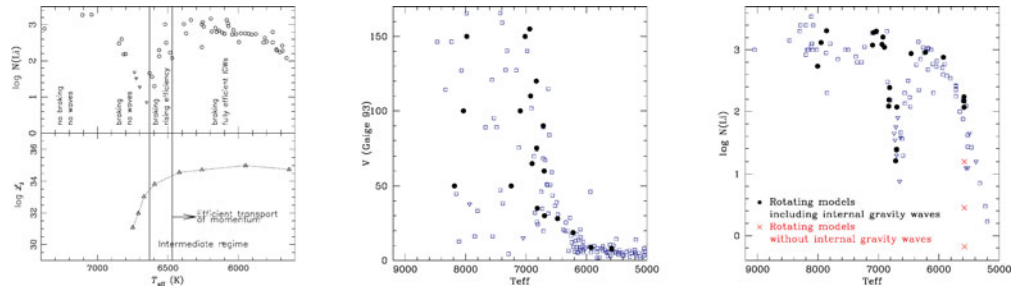

Figure 1. (Left) (*top*) Lithium abundance in the Hyades versus effective temperature. Also indicated are the approximate dependence of surface braking on effective temperature and the requirements for angular momentum transport so that rotational mixing can be expected to lead to the formation of the lithium dip (Talon & Charbonnel 1998). (*bottom*) Filtered angular momentum luminosity of waves below the SLO measuring the efficiency of wave induced angular momentum extraction. Adapted from Talon & Charbonnel (2003). **(Middle)** Projected rotational velocity in the Hyades (Gaigé 1993; open squares and triangles). **(Right)** Li abundances versus effective temperature in the Hyades, Coma B and Praesepe (Burkhart & Coupry 1998, 2000; open squares and triangles). Comparison with our models including IGWs (black dots; Charbonnel *et al.* in preparation); the crosses indicate the predictions for the 1 $M_{\odot}$ computed without IGW

dependence has not been examined in the framework of that model, and no natural relation between the existence of a surface convection zone and an internal poloidal field is expected. Furthermore, recent numerical simulations by Brun & Zahn (2006) have cast doubt on the possibility that such a field would remain confined to the radiative zone for over 4 Gyr (see however the recent results by Wood & McIntyre 2007). Second, Eggenberger *et al.* (2005) studied the impact of the Tayler-Spruit instability in solar models. The impact on light element abundances has not been quantified and once more, no correlation is expected with surface temperature.

The Li data suggest that the efficiency of the additional process is linked to the growth of the convective envelope in stars with effective temperatures around $T_{\rm eff} \simeq 6600$ K. As we shall see below, this is a characteristic of IGWs.

3. IGWs generation and momentum extraction in low-mass stars

In the Earth's atmosphere, wave-induced momentum transport is a key process in the understanding of several phenomena, the best known being the quasi-biennial oscillation of the stratosphere. In astrophysics, IGWs have initially been invoked as a source of mixing for chemicals (Press 1981; Garcia Lopez & Spruit 1991; Schatzman 1993; Montalban 1994; Montalban & Schatzman 1996, 2000; Young *et al.* 2003). Ando (1986) studied the transport of angular momentum associated with standing gravity waves in Be stars. He was the first to clearly state, in the stellar context, that IGWs carry angular momentum from the region where they are excited to the region where they are dissipated. Traveling IGWs have since been invoked as an important source of angular momentum redistribution in single stars (Schatzman 1993; Kumar & Quataert 1997; Talon *et al.* 1997, 2002; Charbonnel & Talon 2005).

3.1. *IGWs generation and wave spectrum*

The existence of IGWs in stars is expected from numerical simulations of penetrative convection both in 2– and 3–D (Hurlburt *et al.* 1986, 1994; Andersen 1994; Nordlund *et al.* 1996; Kiraga *et al.* 2000; Dintrans *et al.* 2005; Rogers & Glatzmaier 2005a, b). Ultimately, one may wish to obtain realistic wave fluxes from such simulations; however, conditions

https://doi.org/10.1017/S1743921308022710 Published online by Cambridge University Press

for these simulations are still too far from realistic to be used at this time (for more details on these aspects see Charbonnel & Talon 2007 and the discussion at the end of the present paper). From a theoretical viewpoint, two different and complementary processes excite IGWs: convective overshooting in a stable region (García López & Spruit 1991; Kiraga *et al.* 2003; Rogers & Glatzmaier 2004), and Reynolds stresses in the convection zone (Goldreich & Kumar 1990; Balmforth 1992; Goldreich *et al.* 1994). Here, we shall use the second mechanism, which has been calibrated on solar p-modes and, thus, seems more reliable at this time. We are fully aware that, as of now, this is the weakest point of wave modeling. Work in underway to evaluate analytically the contribution of penetrative plumes to excitation (Belkacem *et al.* 2008).

For the evolution of angular momentum deep inside the star, the relevant parameter is the net angular momentum luminosity slightly below the convective envelope. To estimate that luminosity, we first need to estimate the spectrum of excited waves. In the Goldreich *et al.* (1994) model that we use, driving is dominated by entropy fluctuations. In our calculations (Talon & Charbonnel 2003, 2004, 2005, 2007, 2008; Charbonnel & Talon 2005), we neglect wave generation by overshooting, although it is expected to be very efficient; our present estimate is thus a lower limit to the correct/total wave flux. As far as numerical simulations are concerned, some authors agree as to the order of magnitude we obtain in our wave-flux (Kiraga *et al.* 2000; Dintrans *et al.* 2005) while Rogers & Glatzmaier (2005) state that we over-estimate this flux. The reason for this discrepancy has been discussed in Charbonnel & Talon (2007), and we are confident that, as 3–D numerical simulations evolve to more realistic regimes, the simulated wave flux will rise with turbulence.

In Talon & Charbonnel (2005), we developed a formalism to incorporate the contribution of IGWs to the transport of angular momentum and chemical elements in stellar models. We showed that the development of a double-peaked shear layer (SLO, for Shear Layer Oscillation), acts as a filter for waves and discussed how the asymmetry of this filter produces momentum extraction from the core when it is rotating faster than the surface. Using only this filtered flux, it is possible to follow the contribution of internal waves over long (evolutionary) time-scales. Let us recall the main features of our formalism. The energy flux per unit frequency $\mathcal{F}_E$ is

$$\mathcal{F}_E\left(\ell,\omega\right) = \frac{\omega^2}{4\pi}\int dr\,\frac{\rho^2}{r^2}\left[\left(\frac{\partial\xi_r}{\partial r}\right)^2 + \ell(\ell+1)\left(\frac{\partial\xi_h}{\partial r}\right)^2\right] \times \exp\left[-h_\omega^2\,\ell(\ell+1)/2r^2\right]\frac{v_c^3 L^4}{1+(\omega\tau_L)^{15/2}}, \tag{3.1}$$

where ξ_r and $[\ell(\ell+1)]^{1/2}\xi_h$ are the radial and horizontal displacement wave-functions, which are normalized to unit energy flux just below the convection zone, v_c is the convective velocity, $L = \alpha_{\rm MLT} H_P$ the radial size of an energy bearing turbulent eddy, $\tau_L \approx L/v_c$ the characteristic convective time, and h_ω is the radial size of the largest eddy at depth r with characteristic frequency of ω or greater ($h_\omega = L\min\{1,(2\omega\tau_L)^{-3/2}\}$). The radial wave number k_r is related to the horizontal wave number k_h by

$$k_r^2 = \left(\frac{N^2}{\sigma^2}-1\right)k_h^2 = \left(\frac{N^2}{\sigma^2}-1\right)\frac{\ell\,(\ell+1)}{r^2} \tag{3.2}$$

where N^2 is the Brunt-Väisälä frequency. In the convection zone, the mode is evanescent and the penetration depth varies as $\sqrt{\ell\,(\ell+1)}$. The momentum flux per unit frequency

https://doi.org/10.1017/S1743921308022710 Published online by Cambridge University Press

$\mathcal{F}_J$ is then related to the energy flux by

$$\mathcal{F}_J\,(m,\ell,\omega) = \frac{2m}{\omega}\mathcal{F}_E\,(\ell,\omega) \tag{3.3}$$

(Goldreich & Nicholson 1989; Zahn, Talon & Matias 1997). We integrate this quantity horizontally to get an angular momentum luminosity

$$\mathcal{L}_J = 4\pi r^2 \mathcal{F}_J \tag{3.4}$$

which, in the absence of dissipation, is conserved (Bretherton 1969; Zahn *et al.* 1997). Each wave then travels inward and is damped by thermal diffusivity and by viscosity. The local momentum luminosity of waves is given by

$$\mathcal{L}_J(r) = \sum_{\sigma,\ell,m} \mathcal{L}_{J\,\ell,m}\,(r_{\rm cz}) \exp\left[-\tau(r,\sigma,\ell)\right] \tag{3.5}$$

where 'cz' refers to the base of the convection zone. τ corresponds to the integration of the local damping rate, and takes into account the mean molecular weight stratification

$$\tau(r,\sigma,\ell) = \left[\ell(\ell+1)\right]^{\frac{3}{2}} \int_r^{r_c} (K_T+\nu_v)\ \frac{N{N_T}^2}{\sigma^4}\left(\frac{N^2}{N^2-\sigma^2}\right)^{\frac{1}{2}}\frac{{\rm d}r}{r^3} \tag{3.6}$$

(Zahn *et al.* 1997). In this expression, ${N_T}^2$ is the thermal part of the Brunt-Väisälä frequency, K_T is the thermal diffusivity and ν_v the (vertical) turbulent viscosity. σ is the local, Doppler-shifted frequency

$$\sigma(r) = \omega - m\left[\Omega(r) - \Omega_{\rm cz}\right] \tag{3.7}$$

and ω is the wave frequency in the reference frame of the convection zone. Let us mention that, in this expression for damping, only the radial velocity gradients are taken into account. This is because angular momentum transport is dominated by the low frequency waves ($\sigma \ll N$), which implies that horizontal gradients are much smaller than vertical ones (*cf.* Eq. 3.2).

When meridional circulation, turbulence, and waves are all taken into account, the evolution of angular momentum follows

$$\rho\frac{\rm d}{{\rm d}t}\left[r^2\Omega\right] = \frac{1}{5r^2}\frac{\partial}{\partial r}\left[\rho r^4 \Omega U\right] + \frac{1}{r^2}\frac{\partial}{\partial r}\left[\rho\nu_v r^4\frac{\partial\Omega}{\partial r}\right] - \frac{3}{8\pi}\frac{1}{r^2}\frac{\partial}{\partial r}\mathcal{L}_J(r), \tag{3.8}$$

(Talon & Zahn 1998) where U is the radial meridional circulation velocity. This equation takes into account the advective nature of meridional circulation rather than modeling it as a diffusive process and assumes a "shellular" rotation (see Zahn 1992 for details). Horizontal averaging was performed, and meridional circulation is considered only at first order. When we calculate the fast SLO's dynamics, U is neglected in this equation. This is justified by the fact that, when shears are large such as in the SLO angular momentum redistribution is dominated by the (turbulent) diffusivity rather than by meridional circulation. However the complete equation is used when secular time-scales are involved as required when we compute full evolution models as in Charbonnel & Talon (2005).

3.2. *Shear layer oscillation (SLO) and filtered angular momentum luminosity*

One key feature when looking at the wave-mean flow interaction is that the dissipation of IGWs produces an increase in the local differential rotation: this is caused by the increased dissipation of waves that travel in the direction of the shear (see Eqs. 3.6 and 3.7). In conjunction with viscosity, this leads to the formation of an oscillating

https://doi.org/10.1017/S1743921308022710 Published online by Cambridge University Press

doubled-peak shear layer that oscillates on a short time-scale (Gough & McIntyre 1998; Ringot 1998; Kumar, Talon & Zahn 1999). This oscillation is similar to the Earth quasi-biennial oscillation that is also caused by the differential damping of internal waves in a shear region.

This SLO occurs if the deposition of angular momentum by IGWs is large enough when compared with (turbulent) viscosity (Kim & MacGregor 2001)†. To calculate the turbulence associated with this oscillation, we rely on a standard prescription for shear turbulence away from regions with mean molecular weight gradients

$$\nu_v = \frac{8}{5} Ri_{\rm crit} K \frac{(r{\rm d}\Omega/{\rm d}r)^2}{{N_T}^2} \tag{3.9}$$

which take radiative losses into account (Townsend 1958; Maeder 1995). This coefficient is time-averaged over a complete oscillation cycle (for details, see TC05).

In the presence of differential rotation, the dissipation of prograde and retrograde waves in the SLO is not symmetric, and this leads to a finite amount of angular momentum being deposited in the interior beyond the SLO. This is the filtered angular momentum luminosity ${\mathcal{L}_J}^{\rm fil}$. Let us mention that in fact, the existence of a SLO is not even required to obtain this differential damping between prograde and retrograde waves, and thus, as long as differential rotation exists at the base of the convection zone, waves will have a net impact of the rotation rate of the interior.

The SLO's dynamics is studied by solving Eq. (3.8) with small time-steps and using the whole wave spectrum while for the secular evolution of the star, one has to use instead the filtered angular momentum luminosity. Let us stress that in the case of the secular evolution we do not follow the SLO dynamics, because of its very short time scale. Rather, we only consider the net angular momentum luminosity beyond the SLO, and its effect on chemicals is given by a local turbulence calculated from a study of the SLO's dynamic over very short time-scales. Let us also mention here that, for both the SLO and the filtered angular momentum luminosity, differential damping is required. Since this relies on the Doppler shift of the frequency (see Eqs. 3.6 and 3.7), angular momentum redistribution will be dominated by the low frequency waves that experience a larger Doppler shift, but that is not so low that they will be immediately damped. Numerical tests indicate that this occurs around $\omega \simeq 1$ μHz.

4. The case of Pop I low-mass stars

A very important property of IGWs is that their generation and efficiency in extracting angular momentum from stellar interiors depend on the structure of their convective envelope, which varies very strongly with the effective temperature of the star. Figure 1 shows the $T_{\rm eff}$-dependence of the filtered angular momentum luminosity of waves below the SLO, which directly measures the efficiency of wave-induced angular momentum extraction, in zero-age main sequence stars around the Li dip. It appears that the net momentum luminosity slightly increases with increasing $T_{\rm eff}$, presents a plateau, and suddenly drops at the $T_{\rm eff}$ of the dip. This clearly indicates that the momentum transport by IGWs has the proper $T_{\rm eff}$-dependence to be the required process to explain the cool side of the Li dip (Talon & Charbonnel 2003).

Talon *et al.* (2002) have shown, in a static model, that waves can efficiently extract angular momentum from a star that has a surface convection zone rotating slower than the interior. Charbonnel & Talon (2005) then calculated the evolution of the internal

† If viscosity is large, a stationary state can be reached.

https://doi.org/10.1017/S1743921308022710 Published online by Cambridge University Press

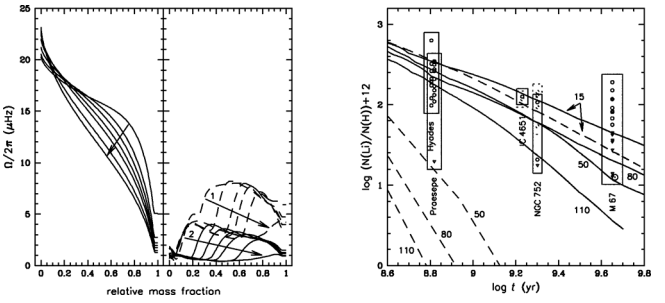

Figure 2. (Left) Evolution of the rotation profile in a solar-mass model with and without IGWs. The initial equatorial rotation velocity is 50 km s^{-1}, and identical surface magnetic braking is applied. (*left*) Model without IGWs. Curves correspond to ages of 0.2, 0.5, 0.7, 1.0, 1.5, 3.0 and 4.6 Gy that increase in the direction of the arrow. Differential rotation remains large at all times. (*right*) When IGWs are included, low-degree waves penetrate all the way to the core and deposit their negative angular momentum in the whole radiative region. Because the core's angular momentum is minute, it is spun down very efficiently. In the so-created "slow" region, damping of retrograde waves increases, leading to the formation of a front, which propagates from the core to the surface. Curves showing propagation of the first front (labeled 1) correspond to ages of 0.2, 0.21, 0.22, 0.23, 0.25 and 0.27 Gy. Further spin down leads to the formation of a second front (ages 0.5, 0.7, 1.0, 1.5, 3.0 and 4.6 Gy). The first front propagates faster than the second one due to stronger braking early in evolution. At the age of the Sun, the radiative region is rotating almost uniformly. From Charbonnel & Talon (2005). **(Right)** Evolution of surface lithium abundance with time for solar-mass stars. The vertical extent of boxes shows the range of lithium values as observed in various galactic clusters for stars with an effective temperature corresponding to that of the model ±100 K at the cluster age, plus a typical error in abundance determination. The horizontal extent corresponds to the age uncertainty. Circles indicate abundance determinations, and triangles denote upper limits for individual stars. The solar value is shown with the usual symbol ⊙. Solid lines correspond to models including IGWs and dashed lines to models without IGWs. Initial velocities are shown on the figure (in km s^{-1}). In the cases without IGWs, except for the slowest rotator, lithium depletion is too strong, by orders of magnitude, at all ages. When included, IGWs, by changing the shape of the internal velocity gradients, lead to a decrease of the associated transport of chemicals. Lithium is then much less depleted and predictions account very well for the data. At all considered ages, the observed dispersion in atmospheric lithium is well explained in terms of a spread in initial velocities. From Charbonnel & Talon (2005).

rotation profile for a solar-mass star with surface spin-down. We showed that, in that case, waves tend to slow down the core, creating "slow" fronts that propagate from the core to the surface (Fig. 2). These calculations confirmed, for the first time in a complete evolution of solar-mass models evolved from the pre-main sequence to 4.6 Gy, that IGWs play a major role in braking the solar core (Charbonnel & Talon 2005). This momentum transport reduces rotational mixing in low-mass stars, leading to a theoretical surface lithium abundance in agreement with observations made in solar mass stars in open clusters of various ages (Fig. 2).

Figure 1 shows our predictions for rotation velocities and Li surface abundances together with the observed data at the age of the Hyades. On the left side of the dip, IGWs play no role and the predictions are taken from Charbonnel & Talon (1999). On the cool side of the dip IGWs are at act and lead to the rise of the surface Li. The model at ∼5800 K corresponds to a 1.0 $M_{\odot}$ star. It was computed for 3 initial rotation velocities of 50, 80 and 110 km s^{-1} both in the case with (black dots) and without IGWs (crosses). Models with IGWs are in perfect agreement with the observations, both regarding the amplitude of the Li depletion and the dispersion at a given effective temperature. More details on these models will be given in Charbonnel *et al.* (in preparation).

https://doi.org/10.1017/S1743921308022710 Published online by Cambridge University Press

5. The case of Pop II low-mass stars

In the context of primordial nucleosynthesis, it has long been debated whether Pop II stars could have depleted their surface Li abundance, just as their metal-rich counterpart did. Recent results on cosmic microwave background anisotropies, and especially those of the WMAP experiment, have firmly established that the primordial Li abundance is ∼2.5 to 3 times higher than the measured Li value in dwarf stars along the so-called Spite plateau (Charbonnel & Primas 2005). The main theoretical difficulty to reproduce these data is that the Li abundance is remarkably constant in halo dwarfs, while it seems at first sight that depletion would lead to a larger dispersion.

A re-examination of Li data in halo stars available in the literature (Charbonnel & Primas 2005) has led for the first time to a very surprising result: the mean Li value as well as its dispersion appear to be lower for the dwarfs than for the subgiant stars. In addition, all the deviant stars, i.e., the stars with strong Li deficiency and those with abnormally high Li content, lie on or originate from the hot side of the Li plateau. These results indicate that halo stars that have now just passed the turnoff have experienced a Li history sightly different from that of their less massive counterparts.

We suggested that such a behaviour is the signature of a transport process for angular momentum whose efficiency changes on the extreme blue edge of the plateau. Such behaviour corresponds to that of the generation and filtering of IGWs in Pop II stars (Talon & Charbonnel 2004), just as it does in the case of Pop I stars. Indeed and as discussed previously, the generation of IGWs and, consequently, their efficiency in transporting angular momentum, depend on the structure of the stellar convective envelope, which in turn depends on the effective temperature of the star (Fig. 1). As in the case of Pop I stars on the red side of the Li dip, the net angular luminosity of IGWs is very high and constant in Pop II stars along the plateau up to $T_{\rm eff} \sim 6300\,{\rm K}$. There, IGWs should dominate the transport of angular momentum and enforce quasi solid-body rotation of the stellar interior on very short timescale. As a result, the surface Li depletion is expected to be independent of the initial angular momentum distribution, implying a very low dispersion of the Li abundance from star to star. In more massive stars however the efficiency of IGWs decreases and internal differential rotation is expected to be maintained under the effect of meridional circulation and turbulence. Consistently, variations of the initial angular momentum from star to star would lead to more Li dispersion and to more frequent abnormalities in the case of the most massive stars where IGWs are not fully efficient, as required by the observations. We note that the mass-dependence of the IGWs efficiency also leads to a natural explanation of fast horizontal branch rotators. The proper treatment of the effects of IGWs together with those of atomic diffusion, meridional circulation and shear turbulence has now to be undertaken in fully consistent models of halo stars.

6. IGWs in intermediate-mass stars

Although waves produced by the surface convection zone can be ignored safely for more massive stars (i.e., with $T_{\rm eff} \geqslant 6700$ K) while on the main sequence, it is not the case for later evolutionary stages. In particular, Talon & Charbonnel (2008) showed that angular momentum transport by IGWs emited by the convective envelope could be quite important in intermediate-mass stars on the pre-main sequence, at the end of the subgiant branch, and during the early-AGB phase. This implies that possible differential rotation, which could be a relic of the star's main sequence history and subsequent contraction, could be strongly reduced when the star reaches the AGB-phase. This could

https://doi.org/10.1017/S1743921308022710 Published online by Cambridge University Press

have profound impact on the subsequent evolution. In particular, this could help solving the long-standing problem of the production of the s-process elements (Herwig *et al.* 2003; Siess *et al.* 2004), as well as explaining the observed white dwarf spins (Suijs *et al.* 2008). Work is in progress to quantify these effects.

Let us also mention that waves can be excited at the boundary of the convective core. These waves travel towards the surface, and are fully damped there, as thermal diffusivity is quite large at the star's surface, and could have a large impact on rotation profiles there (Pantillon, Talon, & Charbonnel 2007). As these stars are fast rotators, the Coriolis force must be accounted for, and much work remains to be done in that direction (Pantillon *et al.* 2007; Mathis *et al.* 2008).

7. Conclusions

IGWs have a large impact on the evolution of low-mass stars, especially through their effect on the rotation profile, which then modifies meridional circulation and shear turbulence. Within this framework, the hydrodynamical models including the combined effects of meridional circulation, shear turbulence and internal gravity waves (using an excitation model that reproduces the solar p-modes) successfully shape both the rotation profile and the time evolution of the surface lithium abundance in low-mass stars. Up to now, no other theoretical model has achieved such a goal. Our comprehensive picture should have implications for other difficult unsolved problems related to the transport of chemicals and angular momentum in stars. We think in particular to the stars on the horizontal and asymptotic giant branches that exhibit unexplained abundance anomalies. No doubt that all these so-called "non-standard" physical processes must be part of the art of modelling stars in the 21st century.

References

Ando, H. 1986, *A&A*, 163, 97
Andersen, B. N. 1994, *Solar Phys.*, 152, 241
Balmforth, N. J. 1992, *MNRAS* 255, 639
Barnes, G., Charbonneau, P., & Mac Gregor, K. B. 1999, *ApJ* 511, 466
Belkacem, K., Talon, S., Goupil, M.-J., & Samadi, R. 2008, *A&A*, in preparation
Boesgaard, A. M. & Tripicco, M. J. 1986, *ApJ*, 302, L49
Boesgaard, A. M. 1987, *PASP* 99, 1067
Bretherton, F. P. 1969, *Quart. J. R. Met. Soc.*, 95, 213
Brown, T. M., *et al.* 1989, *ApJ* 343, 526
Brun, A. S. & Zahn, J. P. 2006, *A&A*, 457, 665
Burkhart, C. & Coupry, M. F. 1998, *A&A* 338, 1073
Burkhart, C. & Coupry, M. F. 2000, *A&A* 354, 216
Chaboyer, N., Demarque, P., Guenther, D. B., & Pinsonneault, M. H. 1995, *ApJ* 446, 435
Charbonneau, P. & Mac Gregor, K. B. 1993, *ApJ* 417, 762
Charbonnel, C. & Primas, F. 2005, *A&A* 442, 961
Charbonnel, C. & Talon, S. 1999, *A&A* 351, 635
Charbonnel, C. & Talon, S. 2005, *Science* 309, 2189
Charbonnel, C. & Talon, S. 2007, AIP Conference Proceedings, Volume 948, pp. 15-26
Charbonnel, C. & Zahn, J. P. 2007a, *A&A* 467, L15
Charbonnel, C. & Zahn, J. P. 2007b, *A&A* 476, L29
Couvidat, S., *et al.* 2003, *ApJ* 597, L77
Deliyannis, C. P., King, J. R., & Boesgaard, A. M. 1997, Kontikas E., *et al.* (eds), *"Wide-field spectroscopy"*, p. 201
Dintrans, B., Brandenburg, A., & Nordlund, A. 2005, *A&A*, 438, 365

https://doi.org/10.1017/S1743921308022710 Published online by Cambridge University Press

Eggenberger, P., Maeder, A., & Meynet, G. 2005, *A&A*, 440, L9
Fossati, L., *et al.* 2008, arXiv0803.3540F
Gaigé, Y. 1993, *A&A* 269, 267
García López, R. J. & Spruit, H. C. 1991, *ApJ* 377, 268
Gebran, M., Monier, R., Richard, O. 2008, arXiv0803.0947G
Goldreich, P. & Kumar, P. 1990, *ApJ* 363, 694
Goldreich, P., Murray, N., Kumar, P. 1994, *ApJ* 424, 466
Goldreich, P. & Nicholson, P. D. 1989, *ApJ* 332, 1079
Gough, D. O. & McIntyre, M. E. 1998, *Nature* 394, 755
Herwig, F., Langer, N., & Lugaro, M. 2003, *ApJ* 593, 1056
Hurlburt, N. E., Toomre, J., & Massaguer, J. M. 1986, *ApJ*, 311, 563
Hurlburt, N. E., Toomre, J., Massaguer, J. M., & Zahn, J. P. 1994, *ApJ*, 421, 245
Kim, E. & MacGregor, K. B. 2001, *ApJ*, 556, L117
Kiraga, M., Jahn, K., Stepien, K., & Zahn, J.-P. 2003, *Acta Astronomica* 53, 321
Kiraga, M., Różyczka, M., Stepien, K., Jahn, K., Muthsam, H. 2000, *Acta Astronomica* 50, 93
Kosovichev, A., *et al.* 1997, *Sol. Phys.* 170, 43
Kumar, P. & Quataert, E. J. 1997, *ApJ* 575, L143
Kumar, P., Talon, S., Zahn, J.-P. 1999, *ApJ* 520, 859
MacGregor, K. & Charbonneau, P. 1999 *ApJ*, 519, 911
Maeder, A. 2005, *A&A*, 299, 84
Maeder, A. & Meynet, G. 2000, *ARAA* 38, 143
Mathis, S., Talon, S., Pantillon, F. P., Zahn, J.-P. 2008, *Solar Phys.*, available online
Matias, J. & Zahn, J.-P. 1998, Provost & Schmider (eds), *"Sounding solar and stellar interiors"*, IAU Symp. 181
Michaud, G. 1986, *ApJ* 302, 650
Montalban, J. 1994 *A&A*, 281, 421
Montalban, J. & Schatzman, E. 1996 *A&A*, 305, 513
Montalban, J. & Schatzman, E. 2000 *A&A*, 354, 943
Nordlund, A., Stein, R. F., & Brandenburg, A. 1996 *Bull. Astron. Soc. of India*, 24, 261
Palacios, A., Talon, S., Charbonnel, C., Forestini, M. 2003, *A&A* 399, 603
Pantillon, F. P., Talon, S., Charbonnel, C. 2007, *A&A* 474, 155
Pasquini, L., Randich, S., Zoccali, M., Hill, V., Charbonnel, & C., Nordström, B. 2004, *A&A* 424, 951
Pilachowski, C. A., Saha, A., & Hobbs, L. M. 1988, *PASP*, 100, 474
Press, W. H. 1981 *ApJ*, 245, 286
Richer, J. & Michaud, G. 1993, *ApJ* 416, 312
Richer, J., Michaud, G., & Turcotte, S. 2000, *ApJ* 529, 338
Ringot, O. 1998, *A&A* 335, 89
Rogers, T. M. & Glatzmaier, G. A. 2005a, *ApJ*, 620, 432
Rogers, T. M. & Glatzmaier, G. A. 2005b, *MNRAS*, 364, 1135
Schatzman, E. 1993 *A&A* 279, 431
Siess, L., Goriely, S., Langer, N. 2004 *A&A* 415, 1089
Suijs, M. P. L., Langer, N., Poelarends, A. J., Yoon, S. C., Heger, A., & Herwig, F. 2008, *A&A* 481, L87
Takeda, Y., Kawanomoto, S., Takada-Hidai, M., & Sadakane, K. 1998, *PASJ* 50, 509
Talon S. 1997 *PhD Thesis*, Université Paris VII
Talon, S. & Zahn J.-P. 1997, *A&A* 317, 749
Talon, S., Kumar, P., & Zahn, J.-P. 2002, *ApJL* 574, 175
Talon, S. & Charbonnel, C. 1998, *A&A* 335, 959
Talon, S. & Charbonnel, C. 2003, *A&A* 405, 1025
Talon, S. & Charbonnel, C. 2004, *A&A* 418, 1051
Talon, S. & Charbonnel, C. 2005, *A&A* 440, 981
Talon, S. & Charbonnel, C. 2008, *A&A* in press, arXiv:0801.4643
Talon, S., Richard, O., Michaud, G. 2006, *ApJ* 645, 634

https://doi.org/10.1017/S1743921308022710 Published online by Cambridge University Press

Talon, S. & Zahn, J. P. 1998, *A&A*, 329, 315
Townsend, 1958
Varenne, O. & Monier, R. 1999 *A&A* 351, 247
Wallerstein, G., Herbig., G. H., & Conti, P.S. 1965, *ApJ*, 141, 610
Wood, T. S., & McIntyre, M. E. 2007, AIP Conference Proceedings, Volume 948, pp. 303-308
Young, P. A., Knierman, K. A., Rigby, J. R., Arnett, D. 2003, *ApJ*, 585, 1114
Zahn, J. P. 1992, *A&A* 265, 115
Zahn, J. P., Talon, S., & Matias, J. 1997, *A&A* 322, 320

Discussion

WOITKE: Why do the simulations of Glatzmaier *et al.* for the excitation of gravity waves by convection fail? Do they yield too strong or too weak convection?

CHARBONNEL: The convective motions in this simulation are "too lazy". The numerical resolution is too small to resolve the hammering of plumes properly. Prandtl-numbers are too low by orders of magnitudes.

KUPKA: I would like to comment on the question of the resolution and turbulence in 3–D global solar simulations. If you take the case of 512^3 grid points, at the bottom of the solar convection zone you have a horizontal resolution of ∼6000 km. The local pressure scale height there is ∼50000 km. So if you consider the energy carrying scales to be of that size, horizontally $R_{eff} \sim (L/R)^{4/3} \sim 20$. Vertically the resolution is perhaps some 600 km, hence $R_{eff} \sim 370$. Also, for comparison, the so-called "extent of overshooting", according to helioseismology, is some 2500 km, if you take it to be $\sim 0.05 H_p$. Thus, the simulations cannot resolve shear-driven turbulence created by the flow on such scales. It is numerically simply too expensive to do that on computers currently available.

LANGER: You prefer g-modes as mechanism to slow down the core of MS stars, since this gives Li-depletion on the cool side of the dip but not on the hot side. Would you not expect a similarly different effect of internal magnetic transport for both sides of the dip, since the cool stars suffer magnetic braking but the hot stars don't?

CHARBONNEL: The question is more related to the transport of angular momentum inside the star, and not to the braking at the surface. For the moment there is no argument to suspect a $T_{\rm eff}$-dependence of the angular momentum transport by magnetic field.

LUDWIG: The Li abundance on the Spite plateau is very homogeneous over almost 1000 K in $T_{\rm eff}$ and 2 orders of magnitude in metallicity. The production rate of gravity waves, and I presume its mixing is dependent on the mass of the convective envelope. Can you comment how the homogeneity of the Li abundance is consistent with the substantial dependence of the stellar structure.

CHARBONNEL: There is in fact a threshold value for the momentum luminosity of waves above which the waves are extremely efficient in transporting angular momentum. The dwarf stars that lie on the Li plateau, despite their slightly different internal structure, all managed to be above that threshold in their infancy. We thus expect that they all managed to become solid-body rotators. As a consequence, they must have depleted Li in a very homogeneous way.